J Neurophysiol 90: 1571–1580, 2003;
10.1152/jn.00392.2003.

Synchrony Levels During Evoked Seizure-Like Bursts in Mouse Neocortical Slices

Wim van Drongelen,[1,2] Henner Koch,[3] Charles Marcuccilli,[1] Fernando Peña,[3] and Jan-Marino Ramirez[3]
Departments of [1]Pediatrics, [2]Neurology, and [3]Organismal Biology and Anatomy, The University of Chicago, Chicago, Illinois 60637

Submitted 21 April 2003; accepted in final form 12 May 2003

van Drongelen, Wim, Henner Koch, Charles Marcuccilli, Fernando Peña, and Jan-Marino Ramirez. Synchrony levels during evoked seizure-like bursts in mouse neocortical slices. *J Neurophysiol* 90: 1571–1580, 2003; 10.1152/jn.00392.2003. Slices ($n = 45$) from the somatosensory cortex of mouse (P8-13) generated spontaneous bursts of activity (0.10 ± 0.05 Hz) that were recorded extracellularly. Multiunit action potential (AP) activity was integrated and used as an index of population activity. In this experimental model, seizure-like activity (SLA) was evoked with bicuculline (5–10 μM) or *N*-methyl-D-aspartate (NMDA, 5 μM). SLA was an episode with repetitive bursting at a frequency of 0.50 ± 0.06 Hz. To evaluate whether SLA was associated with a change in synchrony, we obtained simultaneous intracellular and extracellular recordings ($n = 40$) and quantified the relationship between individual cells and the surrounding population of neurons. During the SLA there was an increase in population activity and bursting activity was observed in neurons and areas that were previously silent. We defined synchrony as cellular activity that is consistently locked with the population bursts. Signal-averaging techniques were used to determine this component. To quantitatively assess change in synchronous activity at SLA onset, we estimated the entropy of the single cell's spike trains and subdivided this measure into network burst-related information and noise-related entropy. The burst-related information was not significantly altered at the onset of NMDA-evoked SLA and slightly increased when evoked with bicuculline. The signal-to-noise ratio determined from the entropy estimates showed a significant decrease (instead of an expected increase) during SLA. We conclude that the increased population activity during the SLA is attributed to recruitment of neurons rather than to increased synchrony of each of the individual elements.

INTRODUCTION

Epilepsy is the most common serious pathological neurologic condition. It affects approximately 50 million people worldwide, with an incidence in developed countries of 50–70 cases per 100,000 (Hauser et al. 1991). A better understanding of epileptogenesis at the cellular and molecular level is crucial because recent studies suggest that nearly 40% of people diagnosed with partial seizures are not controlled with anticonvulsants (Gilliam 2002; Kwan and Brodie 2000; Mattson et al. 1996). From the standpoint of electrophysiology, the ictal state is traditionally associated with synchronized hyperactivity in neural networks and high levels of cellular depolarization (Connors 1984; Gutnick et al. 1982). However, synchronization in the nervous system is not always pathological. In fact, synchronized population activity can be observed during both the sleep and the awake state, and it is one of the hallmarks of information processing in the mammalian nervous system (e.g., Jackson et al. 2003). Consequently, the most important challenges in epilepsy research are to understand the process of ictogenesis and to discriminate between activity occurring during an epileptic state and synchronized activity occurring during other physiological states.

To study burst activity, we performed electrophysiological recordings on neocortical slices of the somatosensory area of mouse. We selected the neocortex because it pertains to the seizures most commonly seen in the clinical setting of pediatric epilepsy. Other researchers have successfully used cortical and hippocampal slice preparations in the study of epilepsy (e.g., Avoli et al. 1987; Bikson et al. 2002; Connors 1984; Connors and Amitai 1993; Dickson and Alonso 1997; Gutnick et al. 1982; Hablitz 1987; Netoff and Schiff 2002; Nishimura et al. 1996; Schwartzkroin 1994) and other state-dependent processes, such as sleep- and wakefulness (Sanchez-Vives and McCormick 2000). The neocortical slice enabled us to perform simultaneous extra- and intracellular recordings in a controlled environment, thus allowing us to examine to what extent a cell is synchronized with its environment—"the network." One of the most common methods of inducing bursting behavior under experimental conditions is the application of pharmacological agents that block synaptic inhibition or mimic an excess of excitatory synaptic input (Connors and Amitai 1993). To decrease inhibition of the network elements, we applied bicuculline, an antagonist of the γ-aminobutyric acid ($GABA_A$) receptor–channel complex. An excess of excitatory input was obtained with *N*-methyl-D-aspartate (NMDA) application to stimulate the excitatory NMDA receptors.

We used averaging techniques to quantify synchrony and a method described by Reich et al. (2001) to estimate different components of entropy of single-unit spike trains. Computation of spike train–related entropy allowed us to quantify the relationship between the activity of individual neurons and the associated network action potential activity. In the experiments, entropy values were obtained *1*) at baseline activity, *2*) during the peak of either bicuculline- or NMDA-induced bursting (a seizure-like transient state), and *3*) at steady state. A small portion of this study was described in a preliminary report (van Drongelen et al. 2003).

Address for reprint requests: Wim van Drongelen, The University of Chicago, Department of Pediatrics, MC 3055, 5841 S. Maryland, Chicago, IL 60637 (E-mail: wvandron@peds.bsd.uchicago.edu).

The costs of publication of this article were defrayed in part by the payment of page charges. The article must therefore be hereby marked "*advertisement*" in accordance with 18 U.S.C. Section 1734 solely to indicate this fact.

METHODS

Neocortical slices

Neonatal (P8-13) male or female CD-1 mice ($n = 25$) were deeply anesthetized with ether and decapitated at the C3/C4 spinal level, and cortex samples were isolated in ice-cold artificial cerebrospinal fluid (ACSF). One hemisphere was then glued onto an agar block with its rostral end up and mounted into a vibrating tissue slicer. Coronal slices (500 μm thick) of the somatosensory cortex were transferred into a recording chamber and submerged under a stream of ACSF (temperature, 30°C; flow rate, 10 ml/min) containing (in mM): 118 NaCl, 3 KCl, 1.5 $CaCl_2$, 1 $MgSO_4$, 25 $NaHCO_3$, 1 NaH_2PO_4, and 30 D-glucose equilibrated with carbogen (95% O_2-5% CO_2). In all experiments, the potassium concentration was routinely raised from 3 to 5 mM over 30 min to obtain spontaneous rhythmic activity close to 0.1 Hz.

Experiments

Here we report results of three types of experiments in which we focused on cellular and network action potential (AP) activities. In one set of recordings ($n = 20$) we evoked seizure-like activity (SLA) with 10 μM bicuculline while recording population and intracellular activity (Fig. 1). In the second set ($n = 20$) the SLA was evoked with 5 μM NMDA and an identical recording setup. In the third type of experiment ($n = 5$) multichannel extracellular activity was recorded. The multichannel electrodes were constructed by mounting micropipettes on a base, and the multiunit recordings used the same amplifier and filter settings as described above. The electrodes in the multielectrode with a spacing of 400 μm were placed in a row of 4 electrodes parallel to the cortical surface. In the multichannel recordings we used 5 μM bicuculline to evoke SLA.

Extracellular signals were amplified 10,000 times, filtered between 0.25 and 1.5 kHz. This resulted in a trace that represented the multiunit AP activity (*top trace*, Fig. 1). This trace was rectified and integrated using an electronic integrator with a time constant of 50 ms ($\int$ in Fig. 1, *B* and *C*). The output of the integrator was used as an index of the surrounding AP activity. Intracellular patch-clamp recordings ($n = 40$) were obtained from neocortical neurons in layers 3–5 with the blind-patch technique. The patch electrodes were manufactured from filamented borosilicate glass tubes (Clarke GC 150TF), filled with a solution containing (in mM): 140 K-gluconic acid, 1 $CaCl_2 \cdot 6H_2O$, 10 EGTA, 2 $MgCl_2 \cdot 6H_2O$, 4 Na_2ATP, 10 HEPES. In 6 experiments, the intracellular pipettes contained biocytin (4.5 mg/ml) to allow for identification of neuron location and morphology. In all cases the identified neurons were pyramidal cells. Electrodes with a positive pressure of 35–50 mmHg were penetrated deep into the slice in 10-μm steps using a piezo-driven micromanipulator (Böhm, Göttingen, Germany). As the electrode approaches the cell, the measured electrode resistance increases. To obtain a Giga seal, we removed the positive pressure and applied negative suction. All recordings were low-pass filtered (0–2 kHz, Bessel 4-pole filter, −3dB). The cells described in this study had membrane potentials ranging from −57 to −72 mV and APs with an overshoot. Because the extracellular and intracellular electrodes were in close proximity of each other (estimated interdistance $\leq$ 150 μm), the integrated extracellular signal was used as an index for the AP activity of the surrounding population (network) of neurons (Fig. 1).

Synchrony, recruitment, and reconfiguration

Multiple ways to quantify synchrony have been described (e.g., Brown and Kocarev 2000), and the definition of a particular synchrony measure in any study should reflect the problem at hand. In our case, we were interested in sustained rhythmic bursts in the neocortical microcircuitry as an underlying process in epileptiform discharges. We therefore determined the single cell's relationship with the network bursting behavior (burst-related window, Fig. 1*B*). Our *synchrony* measure reflects this, and is defined as the component of cellular activity that is consistently locked with the network burst. The phase of this consistently locked component relative to the network may equal any value between 0 and 2π radians. This reflects our assumption that any consistent component of the cellular activity is associated with the processes that generate and sustain network bursting. Under this assumption, the other (*asynchronous*) components of the cell's activity pattern are considered to be *noise* because they reflect different processes that are not locked with the network bursts. Details of our methods to study and quantify synchrony and noise are described in the *Quantitativte analysis* section.

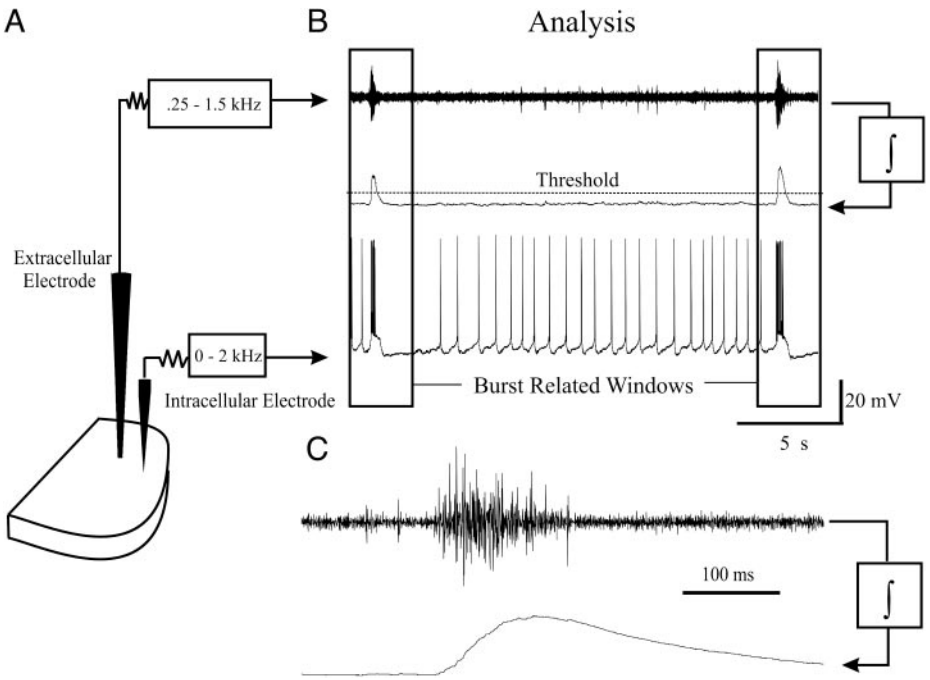

FIG. 1. Recording and data preprocessing. Extracellular and intracellular electrodes were placed in close proximity (*A*), and were used to record network and cellular spike activity (*B*). Network spike activity was rectified and integrated ($\int$) to make network burst activity clearly visible and detectable (*B, middle trace*). *C*: detail of multiunit activity and associated *integrated trace*. Network bursts were detected as integrated signal exceeded threshold adjusted just above noise level (*B, middle trace*). Burst-related window was placed around burst-detection event. Burst-related network and single-cell activities in this window were used for further analysis.

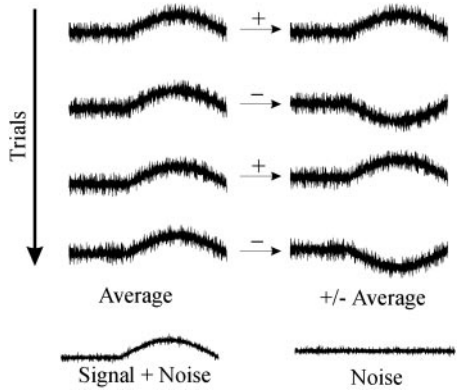

FIG. 2. Example of applied signal-averaging technique. *Left*: averaging over trials can enhance signal-to-noise ratio in a set of trials that contain signal and noise. *Right*: ± average (obtained by inverting all even trials before averaging all trials). Because signals cancel, ± average will contain a noise estimate.

The term *recruitment* is applied to neurons with AP activity that do not show any synchrony with the network during the baseline (BLN) phase before seizure onset, and that become (at least partly) synchronous during SLA. Recruitment can be subdivided into two types.

1) Recruitment in the strict sense (*S-recruitment*) encompasses cells that display no consistently locked network-related AP and/or subthreshold activity during the BLN phase, but become synchronized during SLA onset.

2) Cells that display synchronous subthreshold depolarization during the BLN phase and discharge synchronously during the SLA also become recruited in a broader sense. Because just altering the neuron's excitability could mimic this type of recruitment, we refer to this as *E-recruitment*.

We believe that distinguishing between both types of recruitment (S- and E-recruitment) is critical. Subthreshold activity during the BLN phase will also contribute to field potentials in the EEG; thus E-recruitment is not necessarily associated with dramatic changes in the field potential. In contrast, neurons that are without any network-related activity during the BLN phase, although synchronized during the SLA phase, will alter field potential recordings during the transition.

Our recordings frequently revealed yet another form of network alteration.Neurons inhibited during the network burst during the BLN phase and excited after SLA onset will contribute to a change in EEG and network activity. Although these neurons may remain synchronized with the population activity, their phase of discharge is altered. We hypothesize that this phenomenon is attributedto a drastic change in neuronal processing within cortical networks (e.g., suppression of inhibitory pathways) and we therefore refer to this alteration as *reconfiguration.*

Quantitative analysis

In recordings where cellular AP activity was redistributed after onset of SLA, the changes in the level of synchronization between cellular and network activity were quantified. Units that showed recruitment during SLA were not included in this type of analysis. Bursts of APs generated by the population (network) were detected as the integrated AP activity exceeded a threshold (Fig. 1*B*). This threshold was determined visually in each recording and placed just above the noise level of the integrated signal. The population burst frequency and the area under the curve of the integrated bursts were measured. The product of mean area under the curve and the number of bursts s^{-1} was used as a measure of burst activity in the network per unit time.

Both the network activity and cellular signals were averaged

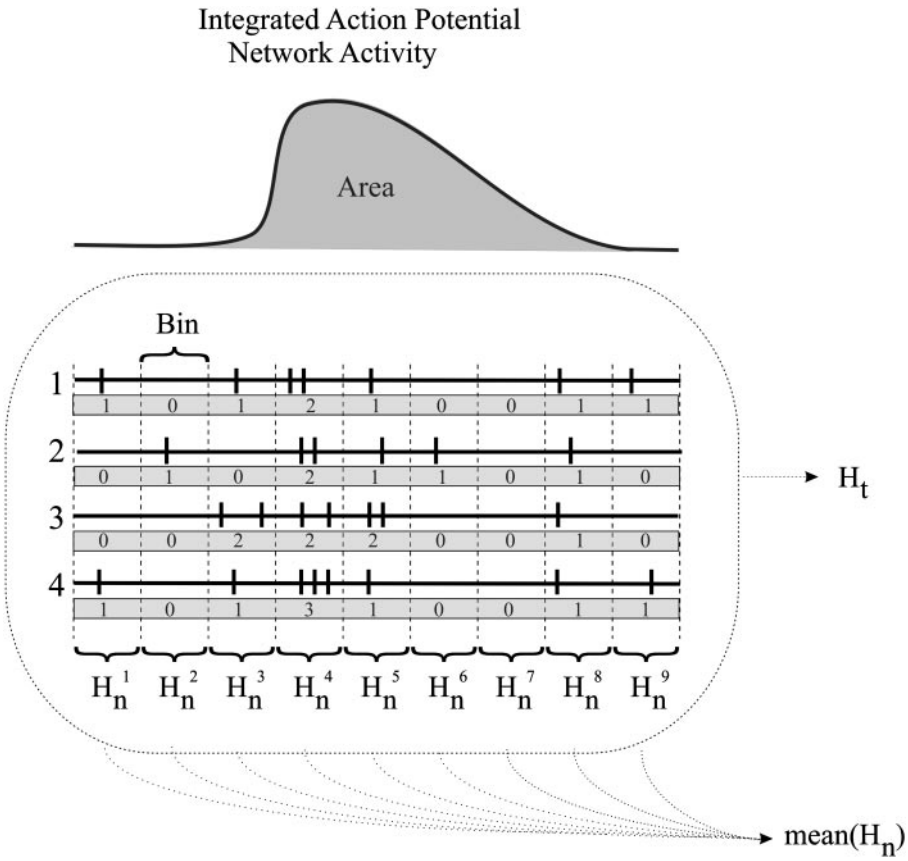

FIG. 3. Population activity measured as integrated multiunit spike trains (*top waveform*). Level of trace indicates ongoing activity level and burst-specific component. Area under curve can be used as burst-related amount of spike activity in underlying network. *Plots 1–4*: spike trains of individual neuron aligned with network burst. Spike trains are subdivided into bins and for each bin we determine number of spikes. From spike counts in bins we can estimate probability (p_i) for each count (i). Entropy values are obtained from estimated probabilities in binned traces. Total entropy (H_t) is obtained from counts in all bins. For each of the bins, noise-related entropy (H_n^j) is determined by variability across trials. Difference between total entropy and mean noise entropy was used to estimate burst-elated information.

using the detected burst onset of the network activity as the trigger. This trigger was placed in the middle of an analysis window (Fig. 1*B*). The activity in the trials was averaged in the usual manner and in a so-called ± *average*. A simulated example of these averaging procedures is shown in the *left* and *right* columns in Fig. 2. In this example the trials contain a consistent and time-locked sinusoidal signal with superimposed random noise. The average process enhances the signal-to-noise ratio by reducing the noise; the end result (the average) contains the signal plus residual noise. In the ± average every other trial is inverted, so that the signal component is cancelled in the end result (Fig. 2). However, the residual noise is still present in the ± averaged result because the estimate of the energy level of random noise in the trials does not depend on whether averaging or ± averaging is used (Schimmel 1967). The amount of residual noise in the average and the ± average is related to the amount of noise in the trials and the square root of the number of trials included in the average. The quotient of the RMS (root mean square) values of the demeaned average and ± average is commonly used as an index for the signal versus noise components. Strictly this ratio is the signal plus noise (S + N) divided by the noise (N) because the average includes both the signal component and the residual noise (Fig. 2). In the following we refer to the RMS ratio as the signal (+ noise)-to-noise ratio. This ratio is a good indicator for the synchronous component, defined as the time-locked component in the signal. For each recording we used the same number of trials in the averages across different bursting patterns and thus we could also use this technique to compare signal (+ noise)-to-noise levels obtained during the different patterns. This ratio was also used for comparison with a signal (+ noise)-to-noise ratio estimated from entropy measures described in the following paragraph. To avoid large effects of nonstationarity as much as possible, analysis was carried out for 10–30 subsequent bursts within each of the states (preseizure, seizure, and postseizure) separately. For each cell the number of trials considered for the analysis was determined by the number of bursts observed during the SLA.

To study network-related information content in the cellular activity, the entropy of the intracellularly recorded spike trains was estimated. The method we applied is identical to the one described by Reich et al. (2001). The only difference was that we aligned the spike trains in the trials according to the population burst (burst-related window, Fig. 1*B*) and not on the basis of an external stimulation or trigger. A simplified example of the procedure is shown in Fig. 3. Here we depict 4 trials aligned with the network burst (*top trace* in Fig. 3). The first step to obtain an entropy value for the cellular AP activity was to divide the spike trains into bins (9 bins in each of the 4 trials in the example of Fig. 3). The distribution of the spike counts in the bins was used as an estimate of the probability (p_i) for each

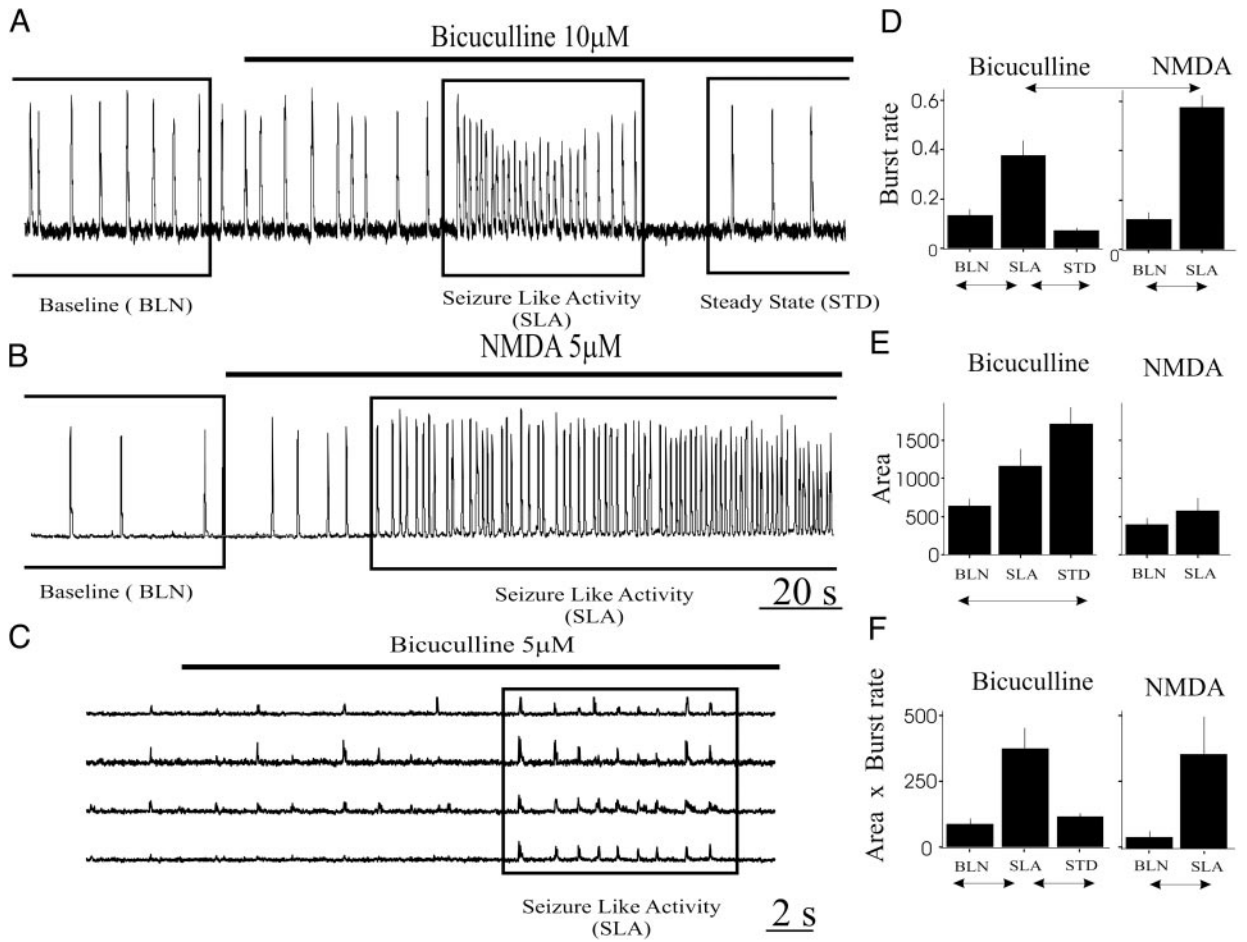

FIG. 4. Result obtained from integrated network action potential (AP) activity. *A*: bicuculline-evoked seizure-like activity (SLA). *B*: *N*-methyl-D-aspartate (NMDA)–evoked SLA. *C*: example of four-channel recording of bicuculline-evoked SLA. At SLA onset, fourth channel becomes involved in bursting activity. *D*: bar graph of mean burst rate (bars represent SE) during different phases for bicuculline experiments (*left*) and NMDA experiments (*right*). *E*: bar graph of mean area under curve of integrated waveform (bars represent SE) during different phases for bicuculline experiments (*left*) and NMDA experiments (*right*). *F*: bar graph of product of *D* and *E*. In *D*, *E*, and *F*, significant differences ($P < 0.05$) are indicated with arrows. Significant difference between SLA states ($P < 0.05$) is indicated with dashed line.

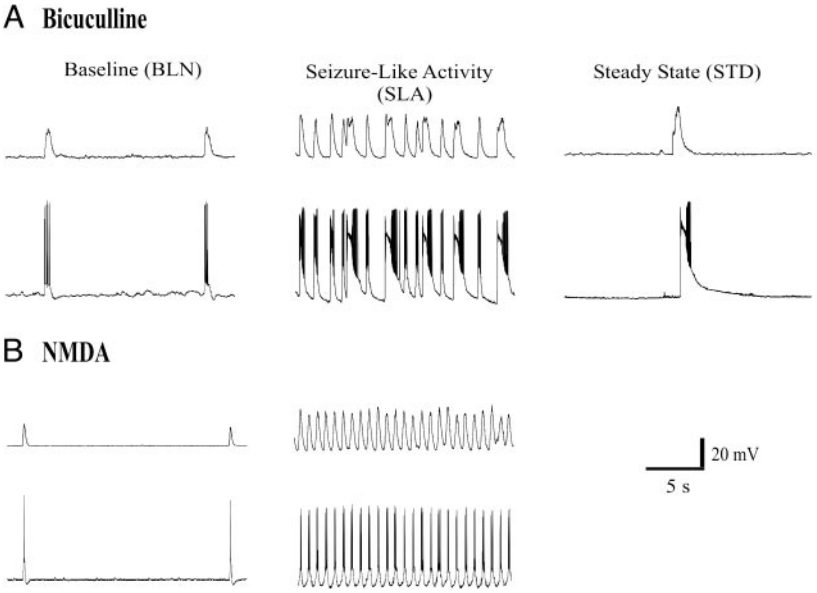

FIG. 5. Two examples showing cellular excitatory activity during multiple network bursts for each phase. In each panel *top* is integrated multiunit activity and *bottom* is intracellular recording. *A*: bicuculline-evoked activity [baseline (BLN), SLA, and steady state (STD)]. *B*: NMDA-evoked activity (BLN and SLA).

observed count (i). In the example of Fig. 3 we have a total of $4 \times 9 = 36$ bins; we observe 15 bins with zero spikes ($p_0 = 15/36$), 15 bins with one spike ($p_1 = 15/36$), 5 bins with two spikes ($p_2 = 5/36$, and 1 bin with three spikes ($p_3 = 1/36$). This probability was used for entropy estimation (H) applying Shannon's formula for entropy as the basis (Reich et al. 2001; Strong et al. 1998)

$$H = -\left[\sum_{i=0}^{\infty} pi\ ^2\log\ (p_i)\right] + B \qquad (1)$$

A bias term B was added to the estimate of the entropy to correct for underestimation. The estimated probabilities derived from the spike counts will differ from the real ones because of the limited number of observations. It was shown by Victor (2000) that an estimate of the bias can be made, by taking the number of observed states (K) and the number of observations (O) into account

$$B = [K - 1]/[2O \ln (2)] \qquad (2)$$

In the example of Fig. 3 we show $4 \times 9 = 36$ observations and 4 different states (0, 1, 2, and 3 spikes per bin: i.e., $O = 36$ and $K = 4$). The total entropy was determined by taking into account all bins, and represents the variability across time (H_t, Fig. 3). The cell's APs that are not locked with the population burst contribute to the variability in the observed spike trains. Spike counts in the bins across trials were used to estimate the noise entropy for each bin j (H_n^j, for the 9 bins in Fig. 3). The mean value of all noise estimates was used as the noise estimate for further analysis. When calculating H_n^j, we frequently encountered subsequent bins with zero value in all trials. As is clear from *Eq. 1*, bins with only zero values do not contribute to the noise entropy estimate and thus potentially lead to an underestimation of this measure. To deal with this issue, we applied the same approach as that of Reich et al. (2001): bins with only zero values were lumped together with the first bin with at least one nonzero value. The entropy estimate for the combined bins was distributed over the grouped bins.

Entropy values were estimated in trials that were aligned with the network burst; therefore *burst-related information* (H_b) could be calculated as the difference between the total and noise entropy

$$H_b = H_t - \text{mean}\,[H_n^j] \qquad (3)$$

Each of the entropy values in *Eq. 3* was determined before, during, and after evoking SLA. We used the quotient of burst-related information and mean noise entropy as a measure for signal-to-noise. In contrast to the RMS ratio determined from the averages, this measure is a true signal-to-noise ratio. To allow comparison between the results obtained with entropy and the averaging technique, we also included an entropy-based ratio of signal (+ noise)-to-noise by dividing the total entropy (H_t = signal + noise) by the noise entropy (mean $[H_n^j]$). We tested bin sizes between 5 and 100 ms and, following Reich et al. (2001), the bin size that generated the highest information rate was used for further analysis. This procedure is justified because

TABLE 1. *Overview of the relationships between the cell's activity and the network bursts during different phases*

Type	Baseline (BLN)	Seizure-Like (SLA)	Steady State (STD)	Characterization	*n*
Bicuculline	Excitation	Excitation, PDS	Excitation, PDS	(E → E)	8
	Inhibition	Excitation + Inhibition	Excitation, PDS	Reconfiguration	5
	Depolarization	Excitation, PDS	Excitation, PDS	E-Recruitment	3
	No activity	Excitation, PDS	Excitation, PDS	S-Recruitment	4
NMDA	Excitation	Excitation, PDS	—	(E → E)	10
	Inhibition	Excitation, PDS	—	Reconfiguration*	4
	Depolarization	Excitation	—	E-Recruitment	3
	No activity	Excitation	—	S-Recruitment	3
Total					40

(E → E) denotes cells that had an excitatory component during the network bursts before and after SLA onset. Excitation + Inhibition indicates a pattern of initial excitation followed by hyperpolarization. PDS, paroxysmal depolarization shift. * Two of the four cells showing reconfiguration with NMDA application became excitatory and synchronized with the network burst; the other two showed excitation without synchrony.

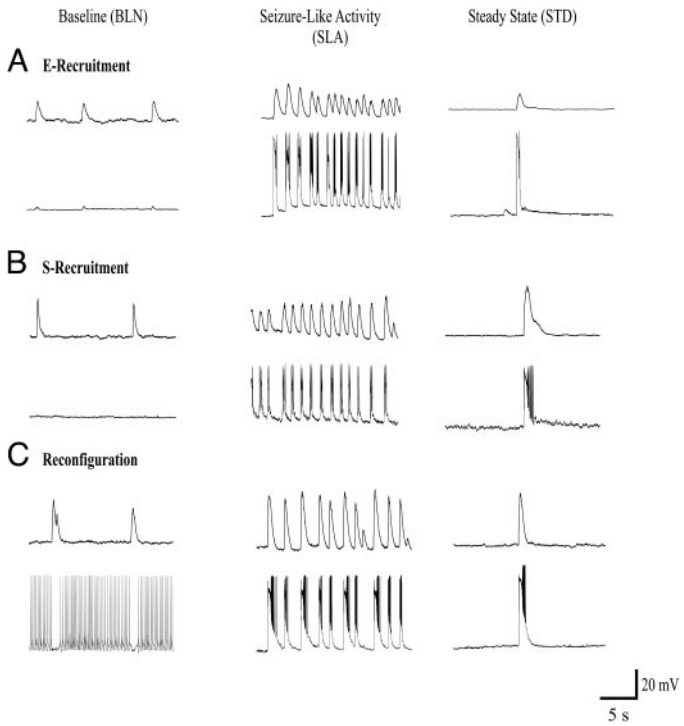

FIG. 6. Three examples of cellular activity before, during, and after bicuculline-evoked SLA. In each panel *top* is integrated multiunit activity and *bottom* is intracellular recording. *A*: E-recruitment. Cell shows subthreshold depolarizations during BLN phase, and AP activity during SLA and STD phases. *B*: S-recruitment. No activity during BLN phase and excitatory AP activity after SLA onset. *C*: reconfiguration. Hyperpolarization associated with network burst during BLN phase, and excitatory activity in other phases.

the real information rate cannot decrease with decreased bin size. Entropy and information values were calculated in bits and were normalized by dividing by the bin size (bits/s).

Other conventional measures of spike activity and similarity between signals such as spike rate and cross-correlation were included in our study. In each phase, a spike rate measure was determined by dividing the total number of spikes in all trials by the total time. Although this is a reliable measure for the level of activity, it does not reflect the distribution of spikes over a time interval such as burst-related entropy does. Cross-correlation (Oppenheim and Schafer 1975) is a linear technique to describe the similarity between two signals and is, as such, a reasonable candidate to investigate synchrony between spike trains of individual cells and population bursts. To evaluate the cross-correlation method as a measure for synchrony, we determined the maximum of the absolute value of the cross-correlation function between the individual spike trains and the integrated network activity.

Change of activity and synchrony measures was evaluated with a Wilcoxon test; differences in measures between the groups where SLA was evoked either by NMDA or bicuculline were evaluated with a Mann–Whitney *U* test. The statistical tests and calculation of the correlation coefficient between measures were performed with SPSS (SPSS, Chicago, IL).

RESULTS

Extracellular burst activity

At a concentration of 5 mM K^+ in the ACSF we observed a baseline (BLN) activity of 0.10 ± 0.05 Hz. After the blockade of GABAergic synaptic transmission with bicuculline (n = 20), the activity changed suddenly and significantly (Fig. 4*A*). Bursts of population activity were generated in trains of 5–30 repetitive bursts at a frequency of 0.40 ± 0.05 Hz, followed by a steady state (STD) of ongoing activity at a frequency of 0.07 ± 0.008 Hz (Fig. 4*A*). The transient activity after adding bicuculline resembles seizure activity and is indicated as seizure-like activity (SLA) throughout the text. A second type of SLA with a burst frequency of 0.60 ± 0.06 Hz was evoked by application of NMDA (n = 20); an STD did not follow these seizures (Fig. 4*B*).

The burst rate of the network is significantly different across stages (Fig. 4*D*, $P < 0.05$) and, compared with the bicuculline-evoked SLA, the increase was significantly higher in the NMDA-evoked SLA ($P < 0.05$, Fig. 4*D*). The average area under the curve of the network burst waveform (as defined in Fig. 3) was significantly increased in the STD compared with that in the BLN ($P < 0.05$, Fig. 4*E*). We calculated the product of area and burst rate to obtain a measure for the network burst activity per unit time; this measure was significantly higher during the SLA compared with that of the other stages in both NMDA- and bicuculline-evoked activity ($P < 0.05$, Fig. 4*F*).

After evoking SLA, multichannel recordings obtained in 5 slices showed an increase in activity and a spread of bursting activity to positions that previously showed low or no activity (Fig. 4*C*). In the example of Fig. 4*C*, 3 of the 4 channels show occasionally synchronized bursting activity before the onset of the SLA. During the SLA, all 4 channels are involved in a series of synchronous burst activity. The multielectrode studies also allowed us to examine the propagation speed of the bursts by determining the interelectrode distance and the time lag between the burst onsets in neighboring electrodes. Interestingly, the average speed (n = 5) of conduction parallel to the cortical surface increased from 10 to 98 mm/s after the onset of a bicuculline-

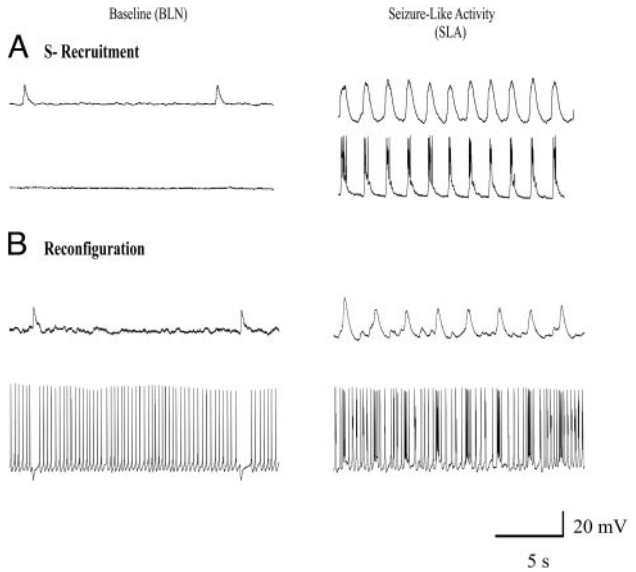

FIG. 7. Two examples of cellular activity across NMDA-evoked SLA. In each panel *top* is integrated multiunit activity and *bottom* is intracellular recording. *A*: S-recruitment. Quiet cell shows excitatory cellular activity after SLA onset. *B*: reconfiguration. Hyperpolarization associated with network burst during BLN phase, and strong excitatory activity during SLA.

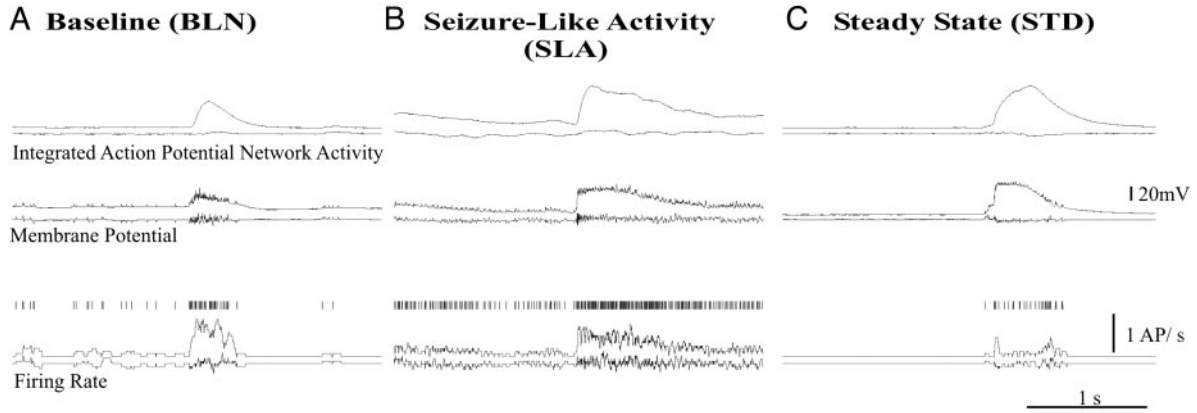

FIG. 8. Example of averaged network and cellular activities during different phases. *A*: BLN, *B*: SLA, and *C*: STD. All averages are based on 16 trials. Population and its associated noise estimate burst (*top*) was used as trigger for averaging procedure. In each phase, the *traces below population burst* represent cell's membrane potential + associated noise estimate, a raster of superimposed action potentials of all trials included in average, and action potential activity (firing rate) + associated noise estimate, respectively. In each phase, cell shows degree of activity that is synchronous with network. Visually, highest degree of synchrony is present in STD.

evoked SLA. Sanchez-Vives and McCormick (2000) found a similar increase of the speed of conduction of AP bursts after blocking the $GABA_A$ receptors in neocortical slices of the ferret.

Relationship between intracellular and extracellular activities

In 40 cases we simultaneously recorded network and cellular activity, and evoked SLA with either bicuculline (Fig. 5*A*, $n = 20$) or NMDA (Fig. 5*B*, $n = 20$). The results are summarized in Table 1. In 18 out of the 40 cells, the baseline activity showed some form of excitation during the network burst, and this relationship remained excitatory after the transition to SLA (E → E in Table 1; Fig. 5). In this E → E group, the excitatory activity during the BLN phase was followed by a hyperpolarization in 3 cases. Thirteen of the 40 neurons did not show any synchronous component during the BLN phase and were recruited after SLA onset (Table 1). Part of this group showed E-recruitment ($n = 6$, change of excitatory level, Fig. 6*A*), whereas the others showed S-recruitment ($n = 7$, Figs. 6*B* and 7*A*). Nine neurons out of the 40 showed inhibition during BLN and excitation after evoking SLA. Examples of reconfiguration are shown in Figs. 6*C* and 7*B*. In the NMDA-evoked SLA, 2 out of the 4 reconfigured neurons showed excitation that was synchronized with the network activity; the other 2 showed excitation without synchrony.

An example of an average relationship (trials = 16) between cellular and network activity is shown in Fig. 8. The *top* (pair) represent the average population burst and the associated noise estimate (± average). The subsequent pair of traces represents the average membrane potential with associated noise estimate. The *bottom* (three) *traces* are a raster plot of superimposed AP activity, the average firing rate and its noise estimate. From the cellular activity depicted in Fig. 8*A* one can conclude that cellular excitation occurs during the population burst, followed by a slight hyperpolarization after the burst. During the SLA (Fig. 8*B*) the maximum depolarization increased slightly, whereas the maximum firing rate decreased (Fig. 8*B*). The STD (Fig. 8*C*) showed a redistribution of the cell's AP activity associated with the network burst. During the BLN and SLA there is a similarity between the average membrane potential and average firing rate waveforms (Fig. 8, *A* and *B*). The relationship comes as no surprise because around AP-threshold levels of the membrane potential, the rate at which APs are generated is a function of the degree of depolarization. However, this similarity is not present in the STD phase because of the occurrence of the paroxysmal depolarization shift (PDS) phenomenon. The PDS changes the membrane potential to depolarization levels that lead to the inactivation of sodium APs.

Quantification

The changes in the total entropy (in bits/s) and cellular activity (in spikes/s) across phases were very similar (Fig. 9, *A* and *B*); both measures are highly correlated ($r = 0.92$, $P < 0.001$). In the bicuculline-evoked activity, the total entropy per unit time shows a significant decrease during the transition from SLA to STD (Fig. 9*B*). By subtracting the noise-related part of the entropy from the total, we determined the component of the entropy that is related to the network burst. Considering the SLA versus BLN, a small but significant increase of burst-related entropy was found in bicuculline-evoked SLA as compared with BLN activity (Fig. 9*C*). No significantly increased burst-related entropy was found in the NMDA-evoked result (Fig. 9*C*). The burst-related entropy during the STD is also significantly increased compared with that of the BLN (Fig. 9*C*). The ratio between the signal (= burst-related activity) and the noise (= activity that is not related to the network burst activity) can be estimated in different ways. We determined this ratio using the averaging and ± averaging technique and by using the entropy estimations. The (S + N)/N ratio between signal + noise and noise as determined by the averaging methods is shown in Fig. 10*A*. Figure 10*B* represents the equivalent (S + N)/N ratio determined from the entropy measures. The data in Fig. 10*C* show signal-to-noise ratios (S/N) determined with the entropy measures. The different measures behaved similarly across phases. The data in Fig. 10, *A* and *B* were comparable and correlated

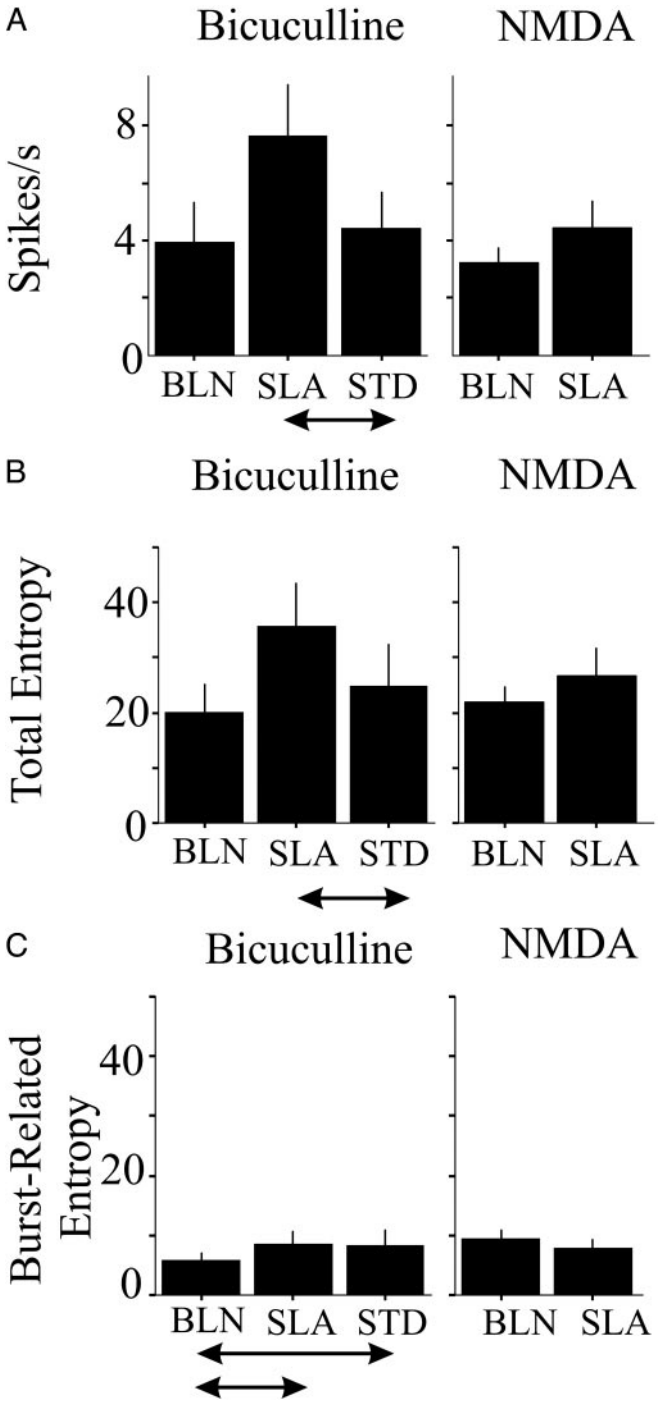

FIG. 9. Histograms of cellular activity measures during different phases for bicuculline-evoked activity (*left*) and NMDA-evoked activity (*right*). Significant differences ($P < 0.05$) indicated by arrows. Bars in histograms represent 1 SE. *A*: mean activity level in spikes/s. *B*: mean total entropy expressed in bits/s. *C*: mean burst-related entropy in bits/s.

($r = 0.64$, $P < 0.001$). Interestingly, the S/N across phases (Fig. 10*C*). In addition, the S/N is significantly decreased during the SLA, compared with that of BLN and STD.

Cross-correlation

The maximum value of the cross-correlation has a tendency to be higher for the more active spike trains even if they are (visually) not as well synchronized with the population bursts as a train with few action potentials. This property of the cross-correlation was confirmed by a significant correlation between the maximum cross-correlation and generic activity measures (spike rate, $r = 0.54$, $P < 0.01$; total entropy, $r = 0.42$, $P < 0.01$; and noise entropy, $r = 0.46$, $P < 0.01$), whereas there was no significant correlation between the maximum cross-correlation and burst-related entropy. The entropy values corresponded well with the results of visual inspection and the signal-averaging technique. Therefore we consider the maximum of the cross-correlation to be not as good a measure for synchrony between AP activity measures of cells and networks as they were defined in this study.

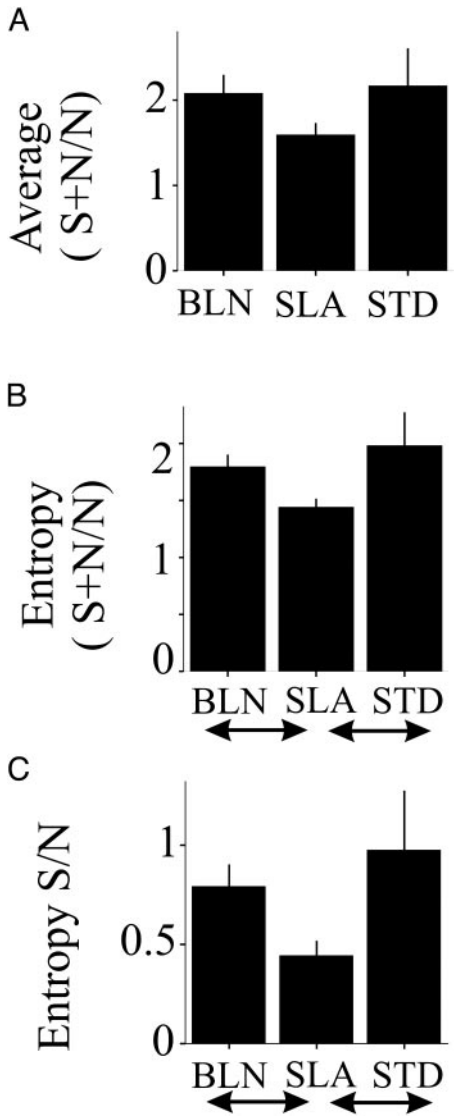

FIG. 10. Signal-to-noise relationships during different phases. Significant differences ($P < 0.05$) indicated by arrows. Bars in histograms represent 1 SE. *A*: mean quotient (S + N)/N between RMS values of average (containing both signal plus noise, Fig. 2) and ± average (containing noise estimate, Fig. 2). *B*: equivalent (S + N)/N ratio, determined from entropy estimates. Total entropy is divided by mean noise estimate (Fig. 3). Both comparable ratios in *A* and *B* are correlated ($r = 0.64$, $P < 0.001$). *C*: mean signal-to-noise ratio (S/N) determined from entropy estimates.

DISCUSSION

Addition of bicuculline or NMDA to the ACSF elicited a seizure-like series of network bursts in mouse neocortical slices. We simultaneously measured population activity and cellular activity from electrodes that were placed in close proximity. This allowed us to study the relationship between the activity of the individual neuron and its surrounding population. The population showed increased underlying activity at onset of the seizure-like state (SLA vs. the other states; Fig. 4*F*), whereas the synchrony measures between the neuron and its associated population showed little or no increase (Fig. 9*C*). The total entropy and cellular activity showed an increase during the SLA (compared with that of the STD; Fig. 9, *A* and *B*). Most of this increased activity was noise related and only a small portion is burst related (to facilitate comparison Fig. 9, *B* and *C* have the same vertical scale). At first sight the conclusions from the intracellular and extracellular data seem contradictory. A massive increase in network synchronous activity was observed (Fig. 4*F*), with no or only a slight increase in burst-related cellular AP activity (Fig. 9*C*). Furthermore, the S/N of the burst-related cellular activity even decreased during the SLA (Fig. 10). Under the assumption that the behavior of the cells we recorded is representative for the population of active units, this finding would be consistent with an increased number of active participants to the network during the SLA. An increase in the number of involved neurons at SLA onset was indeed found (Table 1; Figs. 6 and 7). Here we documented three forms of recruitment. A set of neurons that received no rhythmic synaptic inputs under baseline conditions became prone to bursting in phase with the population discharges at SLA onset (S-recruitment). Activity in several neurons was transformed from sub- to suprathreshold at the transition to SLA (E-recruitment). Another set of neurons that were inhibited became excitatory (reconfiguration).

Recruitment as a mechanism causing the transition to seizure activity was previously described (reviewed by Schwartzkroin 1994). A recruitment mechanism can explain our data and is also supported by the spread of activity observed in the multiarray extracellular measurements after addition of bicuculline (Fig. 4*C*). The low level of synchrony between the individual elements and the active population during the SLA can exist because of the large number of units that participate in the network activity. Intrinsic signal optical imaging studies in slices also show increased and spreading activity after addition of bicuculline in the ACSF (Kohn et al. 2000). Netoff and Schiff (2002) described low synchrony between individual neurons during seizure-like discharges in hippocampal slices. Although in a general sense our findings are compatible with the results of this study, a detailed comparison is difficult. Netoff and Schiff (2002) used a different definition of seizure-like activity and focused on the relationship between the membrane potentials of pairs of cells in which the AP-generating mechanisms were disabled.

An important question is whether rhythmic SLA activity in slices is representative of real seizure activity. There are many reasons to explore the relevancy of the slice model for epilepsy, and conclusions attached to activity patterns should be made cautiously: that is, seizure-like activity in slices is artificially evoked by stimuli that may or may not mimic a truly pathological mechanism; the neocortical slice represents microcircuitry without the influence of other areas; and rhythmic activity itself is not uniquely associated with epileptiform activity because several normal patterns of brain activity can also be characterized as synchronous bursts. Clearly qualifications such as hyperactivity and synchrony cannot separate seizures from nonseizure activity; therefore it seems that quantification of activity levels and synchrony may help us to distinguish between normal and abnormal neural activity and facilitate comparison between slice activity and "in vivo" measurements.

The STD type of population burst evoked by disinhibition of neural networks and the intracellularly recorded paroxysmal depolarization shifts (PDS) are commonly used as experimental models for epileptiform activity (Avoli and Williamson 1996; de Curtis and Avanzini 2001; Gutnick et al. 1982). In most cases this type of activity is considered as a model for the interictal spike. Our findings with bicuculline-evoked activity indicated that the signal-to-noise ratio increased significantly during the STD compared with the SLA (Fig. 10). Some consider the level of synchrony associated with these bursts too high for a credible representation of epileptic events (Schwartzkroin 1994). Our definition of the seizure-like activity is based on the extracellular bursting pattern. To our knowledge, few studies have applied a similar definition. Hablitz (1987) evoked similar discharges with picrotoxin in neocortical slices of young rats and Avoli et al. (1987) induced similar discharges in human neocortical slices at low concentrations of Mg^{2+} in the ACSF. The possibility that the SLA is representative for clinical seizure activity is consistent with data obtained from epilepsy patients who showed low levels of synchronization between single units and the population during seizure activity (Wyler et al. 1982; their Figs. 7, 8, and 9). A study by Babb et al. (1987) reported low levels of synchrony between unitary activity and field potentials recorded with depth electrodes during different seizure types in patients with epilepsy. These findings point in the same direction as our data; that is, seizure onset is associated with low levels of synchrony between active neurons and the average network activity. The recruitment of additional neural network elements may play an essential role in the rhythmic discharges observed in field potentials and the EEG during many seizure types.

We thank Drs. K. E. Hecox, H. C. Lee, D. S. Reich, V. L. Towle, and P. S. Ulinski for valuable comments and discussion.

DISCLOSURES

This work was supported in part by a grant from the Falk Center for Advanced Study and Care of Pediatric Epilepsy.

REFERENCES

Avoli M, Louvel J, Pumain R, and Olivier A. Seizure-like discharges induced by lowering [Mg^{2+}] in the human epileptogenic neocortex maintained in vitro. *Brain Res* 417: 199–203, 1987.

Avoli M and Williamson A. Functional and pharmacological properties of human neocortical neurons maintained in vitro. *Prog Neurobiol* 48: 519–554, 1996.

Babb TL, Wilson CL, and Isokawa-Akesson M. Firing patterns of human limbic neurons during stereoencephalography (SEEG) and clinical temporal lobe seizures. *Electroenceph Clin Neurophysiol* 66: 467–482, 1987.

Bikson M, Baraban SC, and Durand DM. Conditions sufficient for nonsynaptic epileptogenesis in the CA1 region of hippocampal slices. *J Neurophysiol* 87: 62–71, 2002.

Brown R and Kocarev L. A unifying definition of synchronization for dynamical systems. *Chaos*10: 344–349, 2000.

Connors BW. Initiation of synchronized neuronal bursting in neocortex. *Nature* 310: 685–687, 1984.

Connors BW and Amitai Y. Generation of epileptiform discharge by local circuits of neocortex. In: *Epilepsy*, edited by Schwartzkroin PA. New York: Cambridge University Press, 1993, p. 388–423.

Curtis M de and Avanzini G. Interictal spikes in focal epileptogenesis. *Prog Neurobiol* 63: 541–567, 2001.

Dickson CT and Alonso A. Muscarinic induction of synchronous population activity in the entorhinal cortex. *J Neurosci* 17: 6729–6744, 1997.

Gilliam F. Optimizing health outcomes in active epilepsy. *Neurology* 58: S9–S15, 2002.

Gutnick M, Connors B, and Prince DA. Mechanisms of neocortical epileptogenesis in vitro. *J Neurophysiol* 48: 1321–1335, 1982.

Hablitz JJ. Spontaneous ictal-like discharges and sustained potential shifts in the developing rat neocortex. *J Neurophysiol* 58: 1052–1065, 1987.

Hauser WA, Annegers JF, and Urland LT. Prevalence of epilepsy in Rochester, Minnesota 1940–1980. *Epilepsia* 32: 429–445, 1991.

Jackson A, Gee VJ, Baker SN, and Lemon RN. Synchrony between neurons with similar muscle fields in monkey motor cortex. *Neuron* 38: 115–125, 2003.

Kohn A, Metz C, Quibrera M, Tommerdahl MA, and Whitsel BL. Functional neocortical microcircuitry demonstrated with intrinsic signal optical imaging in vitro. *Neuroscience* 95: 51–62, 2000.

Kwan P and Brodie MJ. Early identification of refractory epilepsy. *N Engl J Med* 342: 314–319, 2000.

Mattson RH, Cramer JA, and Collins JF. Prognosis for total control of complex partial and secondarily generalized tonic-clonic seizures. The Department of Veterans Affairs Epilepsy Cooperative Studies No. 118 and No. 264 Group. *Neurology* 47: 68–76, 1996.

Netoff TI and Schiff SJ. Decreased neural synchronization during experimental seizures. *J Neurosci* 22: 7297–7307, 2002.

Nishimura Y, Kitagawa H, Saitoh K, Asahi M, Itoh K, Yoshioka K, Asahara T, Tanaka T, and Yamamoto T. The burst firing in the layer III and V pyramidal neurons of the cat sensorimotor cortex in vitro. *Brain Res* 727: 212–216, 1996.

Oppenheim AV and Schafer RW. *Digital Signal Processing.* Englewood Cliffs, NJ: Prentice-Hall, 1975.

Reich DS, Mechler F, and Victor JD. Formal and attribute-specific information in primary visual cortex. *J Neurophysiol* 85: 305–318, 2001.

Sanchez-Vives M and McCormick DA. Cellular and network mechanisms of rhythmic recurrent activity in neocortex. *Nat Neurosci* 3: 1027–1034, 2000.

Schimmel H. The (±) reference: accuracy of estimated mean components in average response studies. *Science* 157: 92–94, 1967.

Schwartzkroin PA. Cellular electrophysiology of human epilepsy. *Epilepsy Res* 17: 185–192, 1994.

Strong SP, Koberle R, DeRuyter Van Steveninck RR, and Bialek W. Entropy and information in neural spike trains. *Phys Rev Lett* 80: 197–200, 1998.

VanDrongelen W, Koch H, Marcuccilli C, Hecox K, and Ramirez JM. Is burst activity in cortical slices a representative model for epilepsy? *Neurocomputing* 52–54: 963–968, 2003.

Victor JD. Asymptotic bias in information estimates and the exponential (Bell) polynomials. *Neural Comput* 12: 2797–2804, 2000.

Wyler AR, Ojemann GA, and Ward AA. Neurons in human epileptic cortex: correlation between unit and EEG activity. *Ann Neurol* 11: 301–308, 1982.